



Effects of Phonon Scattering on the Performance of Silicon Nanowire

R.Rajesh¹, V.Kanimozhi, A.Nithya³

Assistant Professor, Department of Electronics and Communication Engineering, SKP Engineering College
Tiruvannamalai, Tamilnadu, India^{1,2,3}

ABSTRACT: The effects of phonon scattering on the drain current and performance metrics of a silicon nanowire transistor are studied using a top of the barrier model. When the top of the channel potential is above the source Fermi level, electron backscattering is prohibited by the potential barrier and the transistor operates in near ballistic regime. At higher gate biases, the optical phonon scattering dominates and reduces the ballisticity and performance metrics significantly. The on-state drain current is reduced by 37%, the transconductance is reduced by 63%, and the switching speed is reduced by 60% due to phonon scattering.

KEYWORDS: SiNWFET, MFP, optical phonon, acoustic phonon

I.INTRODUCTION

Scaling of metal-oxide-semiconductor field effect transistor (MOSFET) structures in CMOS technology has enormously improved transistor performance in terms of high switching speed and low power consumption. However, the scaling may not be straightforward in near future due to performance degradation from short channel effects and technology limitations. An alternative device structure, the silicon nanowire (SiNW) transistor has attracted significant attentions to the research community. Their controlled growth down to 3 nm and their applications as field effect transistors, logic gates and sensors have been demonstrated. For transport in nanowire, the free motion of carriers occurs in the longitudinal direction and two-fold quantization occurs in transverse directions. This phenomena decrease the

available scattering states thus tends to increase carrier mobility. However, due to quantization, interaction between carrier and phonon increases and eventually mobility decreases. It has been reported that phonon confinement occurs in silicon nanowire and has been observed using Raman scattering. Numerical simulation shows that onstate current decreases in the presence of acoustic phonons as the device length increases whereas ballistic transport does not have any dependency on device length. Both acoustic phonon and optical phonon scattering reduces carrier mobility. In this work, we have studied the effects of acoustic and optical phonon scattering on the performance of a SiNW transistor using top of the barrier model. The model selfconsistently

calculates the potential at the barrier top, USCF in

the ballistic limit. With the conserved USCF, we then include phonon scattering to calculate the current. The scattering effects turn on when the USCF goes down below the source Fermi level. For a typical value of acoustic phonon mean freepath of 100nm, the ballisticity is reduced by ~ 20% at EF1-

USCF = 0.1 eV, where EF1 is the source Fermi level. At the same value of EF1-USCF, the ballisticity is reduced by ~ 70% for a typical optical phonon mean free path of 10 nm. In the on-state, the current is reduced from 10.56 μ A to 6.56 μ A

when the acoustic and optical phonon scatterings are considered. The transconductance is reduced by 63% and the switching speed by 60%.

International Journal of Advanced Research in Electrical, Electronics and Instrumentation Engineering

(An ISO 3297: 2007 Certified Organization)

Vol. 5, Issue 1, January 2016

II. SIMULATION MODEL

The electrostatics of the model is shown in Fig. 1.

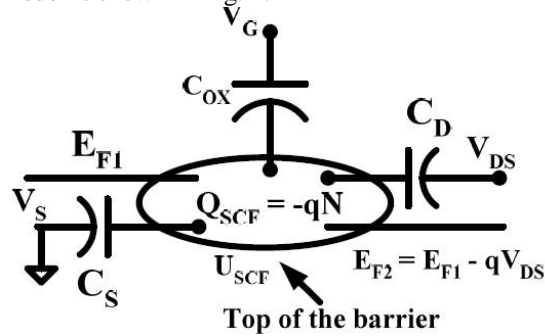


Fig. 1 The electrostatic model of the channel top. The channel top is electrostatically connected to the gate, source, and drain terminals by COX, CS and CD respectively. USCF is the self-consistent channel potential.

The barrier top is connected to the source, drain, and gate by three electrostatics capacitances, CS, CD, and COX, respectively. In terms of the gate and drain control parameters and the charge at the barrier top, the USCF can be written as

$$U_{SCF} = -q(\alpha_G V_{GS} + \alpha_D V_{DS}) + \frac{q^2 AN}{C_T} \dots \quad (1)$$

. VGS and VDS are the gate to source and drain to source biases, respectively. With USCF, the number of electrons per unit length at the barrier top is calculated from

$$N = \frac{1}{2} \int_{U_{SCF}}^{+\infty} D(E - U_{SCF}) [f(E - E_{F1}) + f(E - E_{F2})] dE \dots \quad (2)$$

The factor of 1/2 at the beginning is due to the fact that half of the channel states are filled according to the source Fermi level EF1 and the other half according to the drain Fermi level EF2. The channel density-of-states (DOS) per unit length including spin degeneracy is obtained from

$$D(E - U_{SCF}) = \frac{1}{\pi \hbar} \sqrt{\frac{2m^*}{E - U_{SCF}}} \dots \quad (3)$$

where the equilibrium number of electrons is obtained from Eq. [2] by setting EF1 = EF2 = EF. The equilibrium Fermi level is obtained from the

doping concentration of source and charge neutrality N(EF) – NSD = 0. Eqs. [1] and [2] are self-consistently solved for each bias. Once the self-consistent loop converges, we calculate the drain current including phonon scattering from

$$I = \frac{2q}{h} \int_{U_{SCF}}^{\infty} dE \{ T_S f(E - E_{F1}) - T_D f(E - E_{F2}) \} \dots (4)$$

International Journal of Advanced Research in Electrical, Electronics and Instrumentation Engineering

(An ISO 3297: 2007 Certified Organization)

Vol. 5, Issue 1, January 2016

III. RESULTS

Simulations are performed for a silicon nanowire transistor. The nanowire has a square cross section of width 5 nm and a 2 nm thick SiO₂ gate dielectric. The longitudinal effective mass and band gap of the <100> wire are evaluated from the empirical expressions W is the wire width in nm, m_0 is the mass of a free electron, and the band gap is in eV. The empirical expressions result from the fittings to the sp³d⁵s* atomic orbital basis calculations. To see the effects of phonon mean free path on drain current, we plot the ballisticity versus energy difference $E_{F1} - U_{SCF}$ in Fig. 2. In these plots, the drain to source bias is fixed to 0.5 V and the gate to source bias is varied. The term, ballisticity, is defined by the ratio of incoherent to coherent drain currents. Fig. 2(a) shows the effects of acoustic phonon mean free path on ballisticity and 2(b) shows the effects of optical phonon mean free path on ballisticity. The incoherent drain current with acoustic phonon scattering can be calculated by setting optical phonon mean free path to infinity. Similarly the acoustic phonon mean free path is set to infinity to calculate the drain current with optical phonon scattering. In both acoustic and optical phonon scatterings, the ballisticity is highly dependent on the mean free path. The phonon scattering turns on when the USCF aligns with the source Fermi level or goes down below the source Fermi level. At relatively lower gate biases

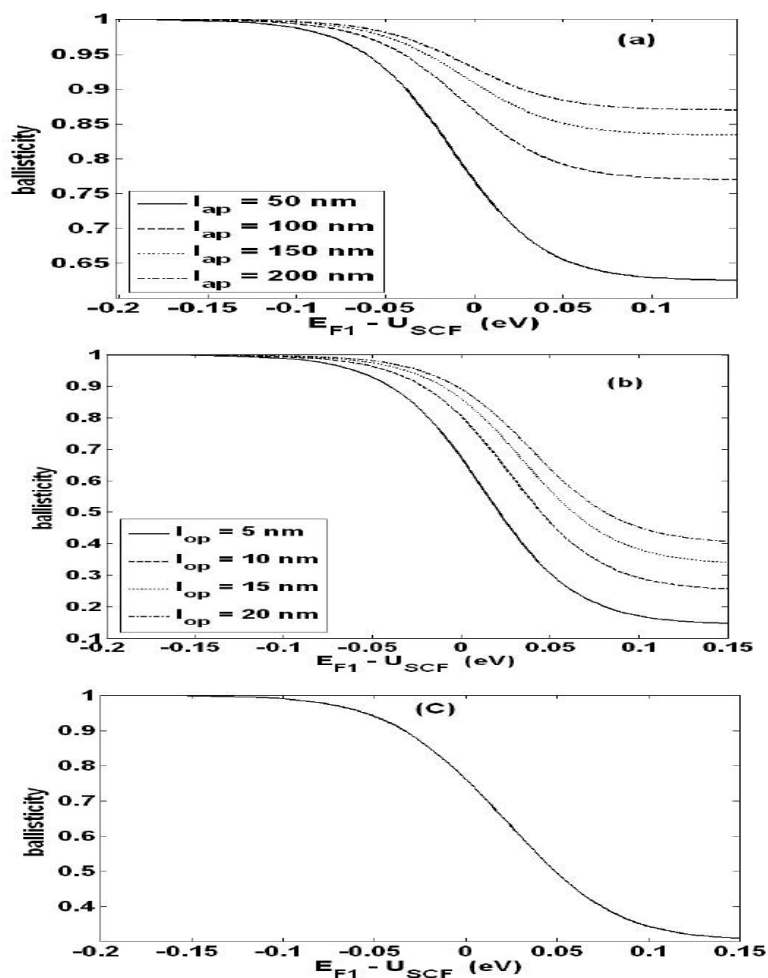


Fig. 2 Ballisticity versus $E_{F1} - U_{SCF}$ plots in the presence of (a) acoustic phonon only, (b) optical phonon only, and (c) both acoustic and optical phonons. The acoustic phonon mean path is 100 nm and the optical phonon mean free path is 10 nm in (c).

($U_{SCF} > E_{F1}$), there exist scattered electrons that cannot go back to the source and the ballisticity does not fall. When U_{SCF} is below the source Fermi level, the scattered electrons can easily go back to the source due to

International Journal of Advanced Research in Electrical, Electronics and Instrumentation Engineering

(An ISO 3297: 2007 Certified Organization)

Vol. 5, Issue 1, January 2016

absence of the potential barrier and the ballisticity is reduced. At these gate biases, the optical phonon scattering is the dominant scattering mechanism due to lower mean free path and lower phonon energy, 0.063 eV. At a energy difference value of 0.1 eV, the ballisticity is reduced by ~ 20% when only acoustic phonon scattering with mean free path of 100 nm is considered. At the same energy difference, the ballisticity is reduced by ~ 70% when only the optical phonon scattering with mean free path of 10 nm is considered. Fig. 2(c) shows the combined effects of acoustic and optical phonon scattering on the ballisticity a potential barrier, and therefore, the electrons that get

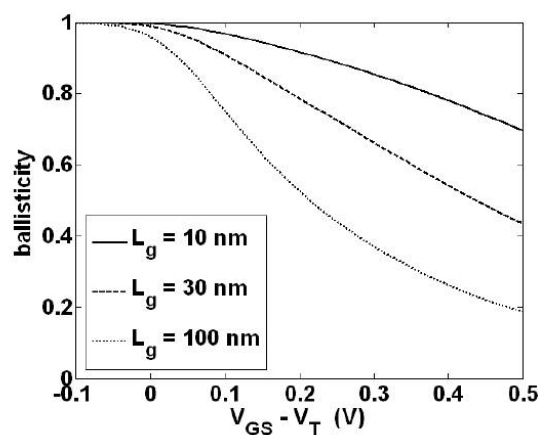


Fig. 3 Comparison of ballisticity for different gate lengths.

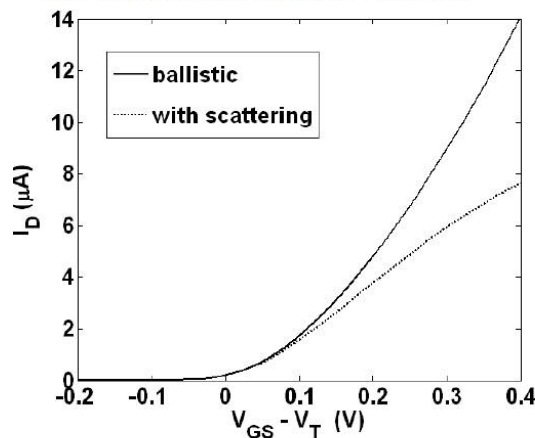


Fig. 4 Comparison of transfer characteristics between ballistic (without scattering) and non-ballistic (with scattering) transport.

In Fig. 3, we show the effects of channel length on

ballisticity in presence of acoustic and optical phonon scattering. Note that the channel is represented by a point in our model and therefore, there is no effect of channel length on USCF. However, the drain current that we calculate with the converged value of USCF depends on the channel length. When the channel length is comparable to the mean free path the transport is near ballistic. The ballisticity is reduced with longer channel which is expected. For quantitative comparison, the ballisticity at on-state is 85% at a channel length of 10 nm. This is reduced to 60% for channel length of 30 nm and to 33% for 100 nm channel. The on-state is defined at the gate bias $V_{GS} = V_T + (2/3)V_{DD}$, where $V_{DD} = 0.5$ V in our simulation and the threshold voltage is the gate voltage at which $USCF = EF1 + KT$. The effects of phonon scattering on the drain current are shown in Figs. 4 and 5. Fig. 4 is the drain current versus gate bias plot with drain bias fixed to 0.5 V and Fig. 5 is the IDVDS

International Journal of Advanced Research in Electrical, Electronics and Instrumentation Engineering

(An ISO 3297: 2007 Certified Organization)

Vol. 5, Issue 1, January 2016

characteristics. In Fig. 4, we see that the phonon scattering has no effect on drain current at the gate overdrive below 0.1 V. At those values of gate overdrive, a finite barrier potential exists and the

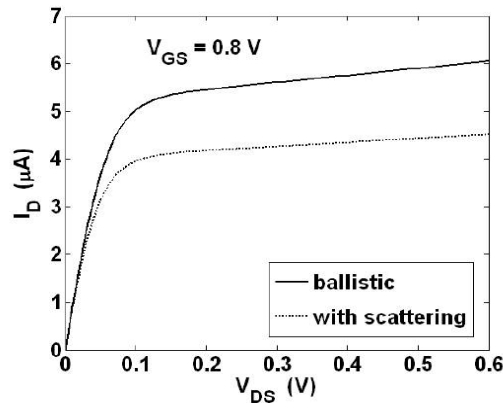


Fig. 5 Drain current versus drain bias plot. Gate bias for this plot is $V_{GS} = 0.8$ V.

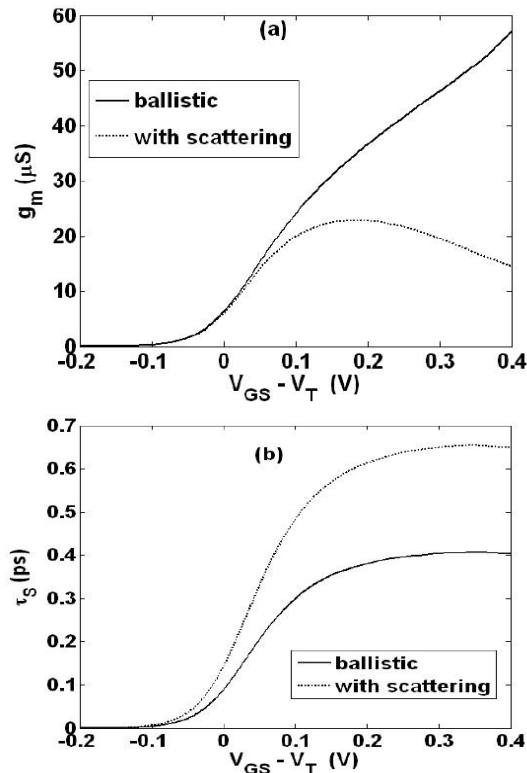


Fig. 6 (a) Transconductance and (b) intrinsic switching delay versus gate bias plot.

scattered electrons can not get back to the source, rather they exit to the drain and the drain current is not affected. In Fig. 5, the gate bias is 0.8 V. At this gate bias, the USCF is 0.0023 eV below the source Fermi level and there is no potential barrier for the scattered electrons to get back to the source. So the phonon scattering reduces the drain current and this effect is stronger at larger drain biases. Finally, we study the effects of phonon



International Journal of Advanced Research in Electrical, Electronics and Instrumentation Engineering

(An ISO 3297: 2007 Certified Organization)

Vol. 5, Issue 1, January 2016

scattering on device performance metrics. The gate capacitance is then obtained from their series combination $C_g = C_{ox}C_Q/(C_{ox}+C_Q)$. Note that the capacitance is obtained from charge and USCF, which, in our model, are calculated in the ballistic self-consistent loop, and therefore, there is no effect of phonon scattering on them. The phonon scattering has the effects on transconductance and switching speed that we calculate from $g_m = dI_D/dV_{GS}$ and $\tau_S = C_g V_{DD}/I_{ON}$. The transconductance and the switching delay are shown in Fig. 6. The phonon scattering strongly affects both the transconductance and switching delay, especially in the onstate. At on-state, the transconductance is degraded from 49.39 μS to 17.89 μS and the switching delay is degraded from 0.406 ps to 0.653 ps.

IV. CONCLUSION

In conclusion, we have used a simple model to study the phonon scattering effects on ballisticity and performance metrics of a silicon nanowire transistor. Due to the presence of a finite barrier, the phonon back scattering is prohibited until the channel potential aligns with the source Fermi level or it goes down below the source Fermi level (low bias). At higher biases, the potential barrier is removed and phonon scattering degrades the ballisticity and device performance mainly due to strong effects of optical phonon. The on-state current is degraded by 36%, the transconductance is degraded by 63%, and the switching delay is degraded by 60% due to phonon scattering.

REFERENCES

- [1] G. Y. Cui, Z. Zhong, D. Wang, W. U. Wang, and C. M. Lieber, "High performance silicon nanowire field effect transistors," NanoLetter, vol. 3, no. 2, pp. 149–152, 2003.
- [2] S. D. Suk, S. Y. Lee, S. M. Kim, E. J. Yoon, M. S. Kim, M. Li, C. W. Oh, K. H. Yeo, S. H. Kim, D. S. Shin, K. H. Lee, H. S. Park, J. N. Han, C. J. Park, J. B. Park, D. W. Kim, D. Park, and B. I. Ryu, "High performance 5 nm radius twin silicon nanowire MOSFET (TSNWFET): Fabrication on bulk Si wafer, characteristics, and reliability," in Proc. IEDM Tech. Dig., 2005, pp. 735–738.
- [3] Y. Wu, Y. Cui, L. Huynh, C. J. Barrelet, D. C. Bell, and C. M. Lieber, "Controlled growth and structures of molecular-scale silicon nanowires," Nano Letter., vol. 4, no. 3, pp. 433–436, 2004.
- [4] H. C. Lin and C. J. Su, "High performance poly-Si nanowire NMOS transistors," IEEE Transaction on Nanotechnology., vol. 6, no. 2, pp. 206–212, 2007
- [5] S. M. Koo, M. D. Edelstein, Q. Li, C. A. Richter, and E. M. Vogel, "Silicon nanowires as enhancement-mode Schottky barrier field effect transistors," Nanotechnology, vol. 16, pp. 1482–1485, 2005.
- [6] J. Wang, A. Rahman, A. Ghosh, G. Klimeck, and M. Lundstrom, "Performance evaluation of ballistic silicon nanowire transistors with atomic-basis dispersion relations," Appl. Phys. Lett., vol. 86, p. 093113, 2005.
- [7] Y. Huang, X. Duan, Y. Cui, L. J. Lauhon, K. H. Kim, and C. M. Lieber, "Logic gates and computation from assembled nanowire building blocks," Science, vol. 294, pp. 1313–1317, 2001.
- [8] Y. Cui, Q. Wei, H. Park, and C. M. Lieber, "Nanowire nanosensors for highly sensitive and selective detection of biological and chemical species," Science, vol. 293, pp. 1289–1292, 2001.
- [9] R. Gupta, Q. Xiong, C. K. Adu, U. J. Kim, and P. C. Eklund, "Laser-Induced Fano Resonance Scattering in Silicon Nanowires" Nano Letters, vol. 3, No. 5, pp. 627–631, 2003.
- [10] M. Frey, A. Esposito, and A. Schenk, "Simulation of intravalley acoustic phonon scattering in silicon nanowires." Solid State Device Research Conference (ESSDERC), 2008 Proceedings of the European [1-4244-2363-5], pp. 258–261, 2008.
- [11] E. B. Ramayya, I. Knezevic, D. Vasileska, and S. M. Goodnick, "Electronic properties of silicon nanowire: Confined phonons and surface roughness." Proceedings of 6th IEEE Conference on Nanotechnology, Cincinnati, Ohio, July 16–20, 2006.
- [12] Tom J. Kazmierski, D. Zhou, Bashir M. Al-Hashimi, and P. Ashburn, "Numerically efficient modelling of CNT transistors with ballistic and non-ballistic effect for circuit simulation." IEEE Transactions on Nanotechnology, Vol. 9, No. 1, 2010
- [13] Mark S. Lundstrom, and J. Guo, "Nanoscale transistors : Device physics, modeling and simulation," Springer, 233 Spring Street, New York, 2006.
- [14] Redwan N. Sajjad, K. Alam, and Q. Khosru, "Parametrization of silicon nanowire effective mass model from $sp^3d^5s^*$ orbital basis calculations," Semiconductor Science and Technology, vol. 24, No. 4, 2009.